Joining of alumina ceramics with Ti and Zr interlayers by spark plasma sintering

Maria Stosz[1,2], Sathya Narayanasamy[1*], Jon Bell[1], Thomas Graule[1], Dariusz Kata[2], Gurdial Blugan[1*]

[1] Empa - Swiss Federal Laboratories for Materials Science and Technology, High Performance Ceramics Laboratory, Ueberlandstrasse 129, 8600 Dübendorf, Switzerland

[2] AGH University of Science and Technology, Faculty of Materials Science and Ceramics, Al. Mickiewicza 30, 30-059 Cracow, Poland

*Corresponding author: Gurdial Blugan (Gurdial.Blugan@empa.ch), Sathya Narayanasamy (Sathya.Narayanasamy@empa.ch)

Abstract

In this study, alumina ceramics were joined by spark plasma sintering technology using zirconium and titanium metals as interlayers. Bonding with Zr was achieved at 800 and 900°C with an applied force of 4.2 kN, and then at 900°C with a force of 3 kN. It was found that Ti bonded to alumina at 700, 800, and 900°C with an applied force of 3 kN. The influence of temperature and pressure on the bonding properties was measured for both interlayers. Scanning Electron Microscope was used to examine the quality of the bonded ceramics and Energy Dispersive X-Ray spectroscopy was used to gain insights into the bonding mechanism. The best joints were obtained at 900°C for Zr and 800°C for Ti. Oxygen diffusion via the formation of oxygen defects/vacancies and the formation of reaction products such as ZrO_2 (and some Ti-Al or TiO_2 reaction products) could underpin the possible bonding mechanisms.

Keywords: Joining ceramics; interlayers; metal interlayers; Spark Plasma Sintering; diffusion bonding;

1. Introduction

Alumina is known for its good thermal conductivity, high-temperature stability, and high strength, and low material and fabrication costs. Therefore, it has many industrial applications in advanced and traditional fields [1], [2].

Alumina ceramics are usually obtained by sintering alumina powders previously formed into a desirable shape [3]. However, this limits its use, because manufacturing objects with large dimensions or complicated shapes becomes difficult [4]. To increase the importance of ceramics in industrial applications, it is necessary to search for new advances in production techniques to overcome the current difficulties. Joining simple alumina components to make more complicated shapes is one of the relatively low-cost solutions [5].

Many ceramic based applications such as solid oxide fuel cells, sensors etc. with complex shapes and composite materials require high performance joining, with properties such as high vacuum tightness, integrity of the joint, chemical durability, stability of the joint at high operating temperatures etc. The popular joining methods for such requirements are solid-state diffusion bonding, active brazing, transient liquid phase bonding, and glass sealing. They are usually based on introducing additional interlayers between the ceramic components [6]–[9]. The achievement of good joints depends not only on the method, but also on the material used to facilitate the joint, i.e., the interlayer. If not chosen carefully, these joints may lead to the failure of the overall ceramic component. Depending on the application, the choice of the interlayer may depend on parameters such as joining temperature, operating temperature, mechanical properties, thermal properties etc. Therefore, it is important to explore different interlayers and joining methods to be able to make robust design choices for such applications.

For high-temperature applications, solid-state diffusion bonding is usually used to join alumina. In this technique, the interlayer does not change its physical state during joining – the interlayer remains solid even at the joining temperature. Furthermore, the mechanisms of joining are similar to the ones occurring during the sintering process of the ceramic material and to interdiffusion [5], [10].

Additional pressure is usually applied during solid-state diffusion bonding to facilitate joining [10]. Also, the temperature is an important parameter, and it is said, to achieve a stable and strong bond, the thermal treatment from the range 0.5 – 0.8 of the melting point of the ceramic component is required [11]. These two factors increase the initial contact between the joining parts, while voids are also created. The next

step of the bonding process is an increase in the contact area, which leads to a reduction of voids. Following this, the diffusion and the reaction start to form the reaction layer [12].

In solid-state diffusion bonding of alumina, metallic interlayers are more commonly used due to several reasons [13]–[16]. First, they can usually diffuse more easily, which can influence the speed of the bonding process [5]. Besides, using a softer metal than the ceramic material can provide better contact between layers due to the plastic deformation of the metallic layer [16]. Literature survey data regarding the use of interlayers to join alumina are presented in Table 1. Among them, titanium is very often applied due to its excellent wettability characteristics on alumina. Besides, it reacts with alumina, forming mostly an intermetallic compound Ti_3Al [17]. Moreover, the Coefficient of Thermal Expansion (CTE) of titanium is around $8.5 \cdot 10^{-6}$ K^{-1}, while the CTE of alumina is around $7 \cdot 10^{-6}$ K^{-1}. The small difference between the CTEs of these two materials can decrease thermal stresses and hence crack formation during cooling, after thermal treatment of bonded systems [18].

Table 1. Examples of systems for solid-state diffusion bonding alumina ceramics from the literature

Substrate	Substrate	Interlayer	Temperature [°C]	Pressure [MPa]	Reference
Alumina	AISI 304	Ti	700, 800, 900, 1000	15	[16]
Alumina	AISI 304	Ti/Mo	800	15	[16]
Alumina	AISI 304	Ti/Cu	800	15	[16]
Alumina	Ti6Al4V	Ag-Cu	750	3	[19]
Alumina	AISI 304	$AlH_3/Mg(AlH_4)_2$	400	20	[20]
Alumina	Cu	Ti-0.8La (wt.%)	350	from 22 to 28	[6]
Alumina	Ti6Al4V	Ti	950, 1000		[14]
Alumina	1Cr18Ni9Ti steel		from 750 to 1200	7	[21]
Alumina	Alumina	Alumina nanopowder	1100	80	[22]
Alumina	Kovar	Al	540	75	[15]
Alumina	TNZ alloy		1175	3	[23]
Alumina	Alumina		1500	69	[24]
Alumina	Ni		1390	4	[25]
Alumina	Cu		1040	5	[13]
Alumina	Pt		1200	1.8	[26]
Alumina	Nb		from 1500 to 1800	from 3 to 15.2	[27]

Besides conventional heating methods, an electric current can be applied to increase the temperature in the system. An example of a method using electric current is Spark Plasma Sintering (SPS), which is gaining more and more interest in ceramic materials treatment [28], [29]. Applying SPS allows to obtain fully-dense ceramics and ceramic-based composites at lower temperatures and it limits the grain growth due to high heating-rates [30]–[34]. SPS was also previously used for sintering alumina ceramics and preparing alumina-

based composites [35]–[38]. Although SPS has been used to join ceramic-based composites using different interlayers, this method was rarely applied to join pure alumina ceramics [39], [40] . One example is the joining of alumina ceramics with B_2O_3 as the interlayer [41].

In this study, alumina ceramics with zirconium and titanium interlayers were joined using SPS. The important properties required for solid-state diffusion bonding indicate that zirconium is a potential candidate for bonding alumina ceramics. First, the wettability of zirconium on alumina is satisfactory [42]. Additionally, its CTE is around $5.9x10^{-6}$ K^{-1}, which is close to that of alumina [43]. Previously, zirconium was only used as an interlayer to join other ceramics, mostly for ZrC_x treatment. It was not used to join alumina despite its good-bonding qualities, while new bonding interlayers are intensively sought for more and more demanding applications [39], [40]. Titanium was chosen since it is one of the more popular interlayer choices for joining alumina as mentioned earlier. However, bonding with Ti interlayer is usually obtained at the temperature between 900-1000°C [14], [16], [44], [45]. During the research, it was hypothesized that the temperature and time of bonding process in the Al_2O_3-Ti-Al_2O_3 system might be decreased, in comparison to the traditional joining methods, by applying the SPS treatment, To our knowledge, this is the first implementation of the SPS technique to join alumina ceramics with metallic interlayers. Some applications have limitations in joining temperatures and dwell times due to the assembly of ceramic based composites with other temperature sensitive matrices. In such cases, SPS might be a possible solution to use appropriate interlayers at lower joining temperatures and lower dwell times.

2. Experimental Methods

Bonding experiments were performed using alumina discs (purity 99.7%, density 99.5%) with a diameter of 10 mm and a height of 1 mm. The linear coefficient of thermal expansion of the used material at room temperature is equal to $7.2 \cdot 10^{-6}$ K^{-1}. A titanium foil with a thickness of 0.1 mm and a purity of 99.6% obtained from Sigma-Aldrich GmbH and a zirconium foil with a thickness of 0.3 mm and a purity of 99.2% obtained from Goodfellow Cambridge Ltd were used as interlayers. Both zirconium and titanium were cut into small discs with a diameter that matched the alumina samples – 10 mm.

The alumina discs were cleaned with acetone and ethanol in an ultrasonic bath for 15 minutes. Four titanium discs and three zirconium discs were cleaned with acetone in an ultrasonic bath for 15 minutes. The three zirconium discs were used in the experiment with higher applied pressure (see Table 2 for details). Three

other zirconium discs were first polished to a surface roughness of < 1 µm and then cleaned with acetone in an ultrasonic bath. These polished discs were used in the experiments with the lower load (see Table 2).

A sandwich structure, where titanium or zirconium foil was placed in-between two alumina discs, was used for each experiment. Graphite foil covered each side of the sandwich structure in order to achieve sufficient electric conductivity through the sample. The samples were then placed between graphite punches in a graphite die and the reaction system was placed in the SPS apparatus. SPS experiments were performed in an FCT System GmbH with a Riedel Precision Cooling System and a Stange Electronik GmbH SE-607 process controller. Graphite dies and punches from STEIMANN CARBON (CH) were used. Thermal treatments were carried out with a pulse lasting 12 ms followed by a 6 ms pause. Experiments were performed under vacuum. The experimental conditions are presented in Table 2. Samples were examined by light microscope (SteREO Discovery.V20 from ZEISS) and Scanning Electron Microscope (SEM) with Energy-Dispersive X-ray (EDX) spectroscopy (Tescan Vega 3 SEM microscope).

3. Results

SPS trials with the zirconium interlayer, under an applied force of 4.2 kN, gave satisfactory results. Joints were obtained at all the tested temperatures. However, the samples cracked on the ceramic side after the experiments, as shown in Figure 1. In the case of the system treated at 1000°C, a part of the ceramic cracked further after a few hours. Among the experiments with the lower force of 3 kN, bonding occurred only at 900°C. No cracks were visible initially. However, after a few hours, the ceramic disc attached to the unpolished side of the zirconium foil fell off. The thermal treatment at 800°C resulted in bonding between zirconium and alumina only on the polished side of the zirconium. The unpolished side did not bond, and the ceramic cracked immediately after the experiment. At 1000°C, the zirconium foil did not bond with alumina ceramic discs on both polished and unpolished sides.

The experiments with the zirconium interlayer gave durable bonds only at 800 and 900°C with an applied force of 4.2 kN. For these samples, the cross-section analysis by SEM was performed (Fig. 2). The joint obtained by sintering at 800°C has low integrity, as gaps between the alumina and the interlayer can be clearly distinguished (Fig. 2a). The joint obtained at the higher temperature of 900°C seems to have a better quality. Zirconium adheres to the ceramic without any visible holes or gaps (Fig. 2b). The unbonded systems and the poorly bonded systems were also examined by SEM-EDX to gain further insights into the spatial distribution of

chemical elements. The EDX analysis was performed for samples treated at 1000°C under both used forces (Fig. 3 and Fig. 4). As it can be seen, traces of zirconium can be found on the alumina surface after both experiments.

The titanium interlayer formed bonds to alumina at 700°C, 800°C and 900°C using the SPS method. Only at 600°C, which is the lowest temperature studied, were non-satisfactory results obtained. Nevertheless, the signs of reaction can be seen on the surface of the metal disc. Moreover, none of the bonded sandwich structures cracked like in previous cases with zirconium as the interlayer. Additionally, the parts remained bonded, and the ceramic did not fall off.

The cross-sections of the joints obtained with the use of titanium interlayer were examined by SEM (Fig. 5). It is evident that treatment at 800°C produces bonding with the best quality and integrity (Fig 5b). Its adherence to the ceramic component is very good as there are no visible gaps between surfaces. At lower and higher temperatures, the quality of the bonding is poorer (Fig 5a, Fig. 5c). The adherence is not good, and the resin used for sample preparation filled the space between the ceramic and the metal.

4. Discussion

During experiments with zirconium, the ceramic discs cracked (Fig. 1). This phenomenon can be caused by different factors. The mismatch between CTE of alumina and zirconium can result in crack formation during heating and cooling cycles. In addition, cracking can be caused by very high cooling rates (> 50°C min^{-1}) typical for the SPS method. Another factor could be the carbon diffusion through the system, as graphite dies, and punches are used. Graphite could accumulate in the ceramic and initiate defects. Moreover, during the joining process, an uneven distribution of the pulse current may occur [46]. The accumulation of energy in one zone can also initiate cracking.

This investigation demonstrates that zirconium could join alumina ceramics. Even unpolished metal can be successfully used for bonding alumina. However, the joints can be achieved only under the application of a high load/pressure. The polished surface can be bonded to alumina under a relatively lower load. Under atmospheric conditions, unpolished zirconium metal is covered by a passive oxide layer, and it is highly possible, that it can influence the reactivity of the system [47]. The reason for this is the general lower reactivity of metal oxides compared to pure metals.

In the experiment with zirconium as an interlayer, the best results were obtained at 900°C for both forces applied (Fig. 2). This suggests that there is only a small range of temperatures in which zirconium bonds with alumina. The previous study showed that the possible reaction route between alumina and Zr can lead to ZrO_2: $Al_2O_3 + 3/2\ Zr \rightarrow 3/2\ ZrO_2 + 2\ Al$. However, at 1100°C, and without additional pressure applied, this reaction is not energetically favorable [48]. Using SPS apparatus makes the components more reactive by applying additional pressure and having electrical current flow through the system. Pressure decreases sintering temperature, while electrical current flow results in a high heating rate of the system due to the occurrence of Joule heating [46]. Running experiments under vacuum can also facilitate bonding because of the oxygen defects forming during the bonding processes [49], [50]. Besides, alumina in the presence of carbon can be decomposed, which gives an additional source of O_2 [51]. The overall Gibbs energy may be reduced because of the above-mentioned reasons and can result in ZrO_2 formation. The effect of ZrO_2 formation on the bonding process is not clear. It may be possible that the formation of a ZrO_2 layer may prevent or slow-down the diffusion of oxygen through the oxide layer. This can help explain why bonding between components is not stable (Fig. 3 and Fig.4), and this is potentially due of the lack of reaction between Al_2O_3 and Zr atoms.

The bonding of alumina ceramic with the use of the titanium interlayer was achieved for the first time by using SPS. The best bond quality was achieved at 800°C. Like the zirconium interlayer, only a specific range of experimental parameters leads to the most successful joining.

Furthermore, with SPS, Ti bonds with alumina at a temperature that is lower than the experiments reported in the literature with more conventional joining methods. Usually, bonding is achieved at 900-1000°C, with the lower pressure applied [14], [52], [53]. Both, higher pressure and the current flow, can decrease the bonding temperature [46]. Moreover, comparing the Ti-Al_2O_3 joint from 800°C (Fig. 5) to the other systems including zirconium after heating at 900°C, it can be said that using titanium metal as an interlayer gives better and more promising results than using zirconium.

The stability of joints is also much better since the systems did not crack apart after a few hours, as was the case with some joints made with zirconium metal, even with the same force applied. Firstly, it can be a result of the lower difference between the CTE of titanium and alumina than for zirconium and alumina. Secondly, SEM images (Fig. 2 and Fig. 5) show that Ti bonds with alumina more strongly than Zr does. It results in a higher free space area between Zr and ceramic specimens, where water vapor from the atmosphere can adsorb at oxygen defect sites and facilitate the breaking of bonds. According to previous research works [48],

[52], [54], alumina can react with titanium as shown below, forming oxide and metallic reaction products such as TiO_2, Ti_3Al, TiAl, and solid solution of oxygen into titanium.

$1/3\ Al_2O_3 + Ti \rightarrow TiO + 2/3\ Al$

$2/3\ Al_2O_3 + Ti \rightarrow TiO_2 + 4/3\ Al$

$Al_2O_3 + 6\ Ti \rightarrow 2\ Ti_3Al + 3\ O_{[Ti]}$

$Al_2O_3 + 2\ Ti \rightarrow 2\ TiAl + 3\ O_{[Ti]}$

5. Conclusion

Zirconium was applied as an interlayer to bond alumina ceramic by using spark plasma sintering. Bonding was achieved, most likely due to the application of spark plasma sintering. The combination of the electric current flow, high pressure, and the creation of oxygen vacancies or defects probably increased the reactivity of the components. However, the process parameters need to be optimized and the method has some disadvantages. First, unpolished metal can be successfully used for bonding alumina, but the applied pressure must be high. Only then, can joining be successfully achieved. Using polished metal surfaces results in joining under a lower load.

The bonding between components is not stable, and this is probably due to the lack of bonding between Al and Zr atoms. Additionally, cracks occur during and after the thermal treatment, most probably due to the mismatch between coefficients of thermal expansions and moisture accumulation in the gaps in bonding.

Bonding achieved with the use of titanium interlayer has good integrity and stability. By applying the spark plasma sintering process, joints were obtained at lower temperatures than usual, i.e. from 700°C. The joining experiment at 600°C resulted just in the oxidation process of titanium without achieving any joining. The cracks did not occur during these experiments. The CTE of alumina is closer to that of titanium metal than zirconium.

The behavior of titanium and zirconium during the bonding process was similar. Both metals created joints only in a specific range of temperature. For zirconium, the ideal bonding temperature was around 900°C, while for titanium it was around 800°C.

In this study, the possibility of bonding alumina to zirconium using SPS was demonstrated, although the joining parameters such as applied pressure and dwell times may be optimized to achieve more stable

joints. SPS is an interesting alternative to traditional joining methods that might expand the options for robust interlayers for specific and challenging ceramic based components.

Acknowledgments

The project was funded by Innosuisse (Application number: 42449.1 IP-ENG).

Availability of data

All data generated or analyzed during this study are included in the article. Further details may be provided by the corresponding author upon reasonable request.

Competing interests

The authors declare that they have no competing interests.

Author contributions

Conceptualization, S.N., M.S., and G.B.; Methodology, S.N. and G.B.; Validation, T.G., D.K. and G.B.; Formal analysis, M.S.; Investigation, M.S.; Experimentation, M.S., J.B.; Writing—original draft preparation, M.S.; Writing—review and editing, S.N., J.B., G.B., T.G., and D.K.; supervision, S.N., G.B., T.G., and D.K.; project administration, G.B.; funding acquisition, G.B.

Bibliography

[1] A. Ruys, 1 - Introduction to alumina ceramics, Woodhead Publishing Series in Biomaterials, A. B. T.-A. C. Ruys, Ed. Woodhead Publishing (2019) 1–37.

[2] B. BEN-NISSAN, A. H. CHOI, and R. CORDINGLEY, 10 - Alumina ceramics, in Woodhead Publishing Series in Biomaterials, T. B. T.-B. and their C. A. Kokubo, Ed. Woodhead Publishing (2008) 223–242.

[3] M. MUNRO, Evaluated Material Properties for a Sintered alpha-Alumina, J. Am. Ceram. Soc. 80(8) (1997) 1919–1928. doi: https://doi.org/10.1111/j.1151-2916.1997.tb03074.x.

[4] W. B. Hanson, K. I. Ironside, and J. A. Fernie, Active metal brazing of zirconia, Acta Mater. 48(18) (2000) 4673–4676. doi: https://doi.org/10.1016/S1359-6454(00)00256-1.

[5] R. W. Messler, 9 - CERAMIC AND GLASS ATTACHMENT SCHEMES AND ATTACHMENTS, R. W. B. T.-I. M. A. Messler, Ed. Burlington, Butterworth-Heinemann (2006) 239–277.

[6] C.-M. Lin and T.-P. Hsins, Facilitating low-temperature diffusion bonding between oxygen-free Al2O3 ceramic and pure Cu through inclusion of 0.8 La (wt.%) to Ti pre-metallized interlayer: Microstructural evolution, metallurgical reactions, and mechanical properties, Surfaces and Interfaces, 21 (2020) 100738. doi: https://doi.org/10.1016/j.surfin.2020.100738.

[7] S. S. Sayyedain, H. R. Salimijazi, M. R. Toroghinejad, and F. Karimzadeh, Microstructure and mechanical properties of transient liquid phase bonding of Al2O3p/Al nanocomposite using copper interlayer, Mater. Des. 53 (2014) 275–282. doi: https://doi.org/10.1016/j.matdes.2013.06.074.

[8] K. Suganuma, T. Okamoto, M. Koizumi, and M. Shimada, Method for preventing thermal expansion mismatch effect in ceramic-metal joining, J. Mater. Sci. Lett. 4(5) (1985) 648–650. doi: 10.1007/BF00720057.

[9] S. Y. Chang, Y. T. Hung, and T. H. Chuang, Joining alumina to inconel 600 and UMCo-50 superalloys using an Sn10Ag4Ti active filler metal, J. Mater. Eng. Perform. 12(2) (2003) 123–127. doi: 10.1361/105994903770343240.

[10] A. Passerone and M. L. Muolo, Joining Technology in Metal-Ceramic Systems, Mater. Manuf. Process. 15 (2000) 631–648.

[11] O. M. Akselsen, Diffusion bonding of ceramics, J. Mater. Sci. 27(3) (1992) 569–579. doi: 10.1007/BF02403862.

[12] Nicholas, M.G., Joining of Ceramics, Materials Science and Technology, eds R.W. Cahn, P. Haasen and E.J. Kramer (2006). https://doi.org/10.1002/9783527603978.mst0204

[13] K. A. Rogers, K. P. Trumble, B. J. Dalgleish, and I. E. Reimanis, Role of Oxygen in Microstructure Development at Solid-State Diffusion-Bonded Cu/α-Al2O3 Interfaces, J. Am. Ceram. Soc. 77(8) (1994) 2036–2042. doi: https://doi.org/10.1111/j.1151-2916.1994.tb07094.x.

[14] Silva, M., Jr., Ramos, A.S., Simões, S., Joining Ti6Al4V to Alumina by Diffusion Bonding Using Titanium Interlayers, Metals 11 (2021) 1728. https://doi.org/10.3390/met11111728

[15] S. Das, A. N. Tiwari, and A. R. Kulkarni, Thermo-compression bonding of alumina ceramics to metal, J. Mater. Sci. 39(10) (2004) 3345–3355. doi: 10.1023/B:JMSC.0000026935.18466.4b.

[16] D. Travessa, M. Ferrante, and G. den Ouden, Diffusion bonding of aluminium oxide to stainless steel using stress relief interlayers, Mater. Sci. Eng. A 337(1) (2002) 287–296. doi: https://doi.org/10.1016/S0921-5093(02)00046-1.

[17] A. K. Misra, Reaction of Ti and Ti-Al alloys with alumina, Metall. Trans. A 22(3) (1991) 715–721. doi: 10.1007/BF02670294.

[18] P. Hidnert, Thermal expansion of titanium, J. Res. Natl. Bur. Stand. (1934). 30 (1943) 101.

[19] M. I. Barrena, L. Matesanz, and J. M. G. de Salazar, Al2O3/Ti6Al4V diffusion bonding joints using Ag–Cu interlayer, Mater. Charact. 60(11) (2009) 1263–1267. doi: https://doi.org/10.1016/j.matchar.2009.05.007.

[20] N. Hosseinabadi, R. Sarraf-Mamoory, and A. Mohammad Hadian, Diffusion bonding of alumina using interlayer of mixed hydride nano powders, Ceram. Int. 40(2) (2014) 3011–3021. doi: https://doi.org/10.1016/j.ceramint.2013.10.006.
[21] H. Rong, Diffusion bonding behaviour of austenitic stainless steel containing titanium and alumina, J. Mater. Sci. 27(23) (1992) 6274–6278. doi: 10.1007/BF00576272.
[22] H. Ferkel and W. Riehemann, Bonding of alumina ceramics with nanoscaled alumina powders, Nanostructured Mater. 7(8) (1996) 835–845. doi: https://doi.org/10.1016/S0965-9773(96)00055-4.
[23] H. Bian *et al.*, Diffusion bonding of implantable Al2O3/Ti-13Nb-13Zr joints: Interfacial microstructure and mechanical properties, Mater. Charact. 184 (2022) 111665. doi: https://doi.org/10.1016/j.matchar.2021.111665.
[24] C. E. Scott and J. A. Brewer, Bend Strengths for Diffusion-Bonded Al2O3, J. Am. Ceram. Soc. 69(8) (1986) C-178-C-179. doi: https://doi.org/10.1111/j.1151-2916.1986.tb04830.x.
[25] K. P. Trumble and M. Rühle, The thermodynamics of spinel interphase formation at diffusion-bonded Ni/Al2O3 interfaces, Acta Metall. Mater. 39(8) (1991) 1915–1924. doi: https://doi.org/10.1016/0956-7151(91)90160-3.
[26] Y.-C. Lu, R. Dieckmann, and S. L. Sass, Formation of a new aluminum oxide with the composition AlO2 by interfacial reaction between Pt and α-Al2O3, Acta Metall. Mater. 42(4) (1994) 1125–1137. doi: https://doi.org/10.1016/0956-7151(94)90129-5.
[27] S. Morozumi, M. Kikuchi, and T. Nishino, Bonding mechanism between alumina and niobium, J. Mater. Sci. 16(8) (1981) 2137–2144. doi: 10.1007/BF00542374.
[28] R. Kuliiev *et al.*, Spark Plasma Sintered B(4)C-Structural, Thermal, Electrical and Mechanical Properties., Mater. (Basel, Switzerland) 13(7) (2020) 1612. doi: 10.3390/ma13071612.
[29] J. Dusza *et al.*, Hot pressed and spark plasma sintered zirconia/carbon nanofiber composites, J. Eur. Ceram. Soc. 29(15) (2009) 3177–3184. doi: https://doi.org/10.1016/j.jeurceramsoc.2009.05.030.
[30] T. P. Nguyen *et al.*, Role of nano-diamond addition on the characteristics of spark plasma sintered TiC ceramics, Diam. Relat. Mater. 106 (2020) 107828. doi: https://doi.org/10.1016/j.diamond.2020.107828.
[31] T. P. Nguyen *et al.*, Electron microscopy investigation of spark plasma sintered ZrO2 added ZrB2–SiC composite, Ceram. Int. 46(11) Part B (2020) 19646–19649. doi: https://doi.org/10.1016/j.ceramint.2020.04.292.
[32] A. Sabahi Namini *et al.*, Role of TiCN addition on the characteristics of reactive spark plasma sintered ZrB2-based novel composites, J. Alloys Compd. 875 (2021) 159901. doi: https://doi.org/10.1016/j.jallcom.2021.159901.
[33] F. Shayesteh, S. A. Delbari, Z. Ahmadi, M. Shokouhimehr, and M. Shahedi Asl, Influence of TiN dopant on microstructure of TiB2 ceramic sintered by spark plasma, Ceram. Int. 45(5) (2019) 5306–5311. doi: https://doi.org/10.1016/j.ceramint.2018.11.228.
[34] B. Nayebi, S. A. Delbari, M. Shahedi Asl, E. Ghasali, N. Parvin, and M. Shokouhimehr, A nanostructural approach to the interfacial phenomena in spark plasma sintered TiB2 ceramics with vanadium and graphite additives, Compos. Part B Eng. 222 (2021) 109069. doi: https://doi.org/10.1016/j.compositesb.2021.109069.
[35] R. Voytovych, F. Robaut, and N. Eustathopoulos, The relation between wetting and interfacial chemistry in the CuAgTi/alumina system, Acta Mater. 54(8) (2006) 2205–2214. doi: https://doi.org/10.1016/j.actamat.2005.11.048.
[36] Y. Tamura, B. M. Moshtaghioun, D. Gomez-Garcia, and A. D. Rodríguez, Spark plasma sintering of fine-grained alumina ceramics reinforced with alumina whiskers, Ceram. Int. 43(1) Part A (2017) 658–663. doi: https://doi.org/10.1016/j.ceramint.2016.09.210.
[37] D. Chakravarty, H. Ramesh, and T. N. Rao, High strength porous alumina by spark plasma sintering, J. Eur. Ceram. Soc. 29(8) (2009) 1361–1369. doi:

https://doi.org/10.1016/j.jeurceramsoc.2008.08.021.
[38] Y. Shi, W. Chen, L. Dong, H. Li, and Y. Fu, Enhancing copper infiltration into alumina using spark plasma sintering to achieve high performance Al2O3/Cu composites, Ceram. Int. 44(1) (2018) 57–64. doi: https://doi.org/10.1016/j.ceramint.2017.09.062.
[39] R. Pan *et al.*, Cross-diffusion phenomena within a ZrCx – Zr – ZrCx joint, J. Eur. Ceram. Soc. 37(8) (2017) 2779–2786. doi: https://doi.org/10.1016/j.jeurceramsoc.2017.02.051.
[40] R. Pan *et al.*, Design of the multiple transition metals interlayer process to diffusion bond ZrCx ceramics, Mater. Des. 137 (2018) 47–55. doi: https://doi.org/10.1016/j.matdes.2017.10.027.
[41] L.-L. Zhu *et al.*, Alumina ceramics joined with screen-printed B2O3 by spark plasma sintering, Ceram. Int. 47(21) (2021) 30838–30843. doi: https://doi.org/10.1016/j.ceramint.2021.07.264.
[42] R. E. Loehman, F. M. Hosking, B. Gauntt, P. G. Kotula, and P. Lu, Reactions of Hf-Ag and Zr-Ag alloys with Al2O3 at elevated temperatures, J. Mater. Sci. 40(9) (2005) 2319–2324. doi: 10.1007/s10853-005-1952-5.
[43] R. B. Russell, Coefficients of Thermal Expansion for Zirconium, JOM 6(9) (1954) 1045–1052. doi: 10.1007/BF03398344.
[44] N. DANDAPAT, S. GHOSH, K. S. PAL, S. DATTA, and B. K. GUHA, Thermal cycling behavior of alumina-graphite brazed joints in electron tube applications, Trans. Nonferrous Met. Soc. China 24(6) (2014) 1666–1673. doi: https://doi.org/10.1016/S1003-6326(14)63239-8.
[45] J. Lemus-Ruiz, A. O. Guevara-Laureano, J. Zarate-Medina, A. Arellano-Lara, and L. Ceja-Cárdenas, Interface behavior of Al2O3/Ti joints produced by liquid state bonding, Appl. Radiat. Isot. 98 (2015) 1–6. doi: https://doi.org/10.1016/j.apradiso.2015.01.010.
[46] Z.-Y. Hu, Z.-H. Zhang, X.-W. Cheng, F.-C. Wang, Y.-F. Zhang, and S.-L. Li, A review of multi-physical fields induced phenomena and effects in spark plasma sintering: Fundamentals and applications, Mater. Des. 191 (2020) 108662. doi: https://doi.org/10.1016/j.matdes.2020.108662.
[47] M. Sowa *et al.*, Characterisation of anodic oxide films on zirconium formed in sulphuric acid: XPS and corrosion resistance investigations, J. Solid State Electrochem. 21(1) (2017) 203–210. doi: 10.1007/s10008-016-3369-2.
[48] R. E. Loehman and A. P. Tomsia, Reactions of Ti and Zr with AlN and Al2O3, Acta Metall. Mater. 40 (1992) S75–S83. doi: https://doi.org/10.1016/0956-7151(92)90266-H.
[49] M. Hajihashemi, M. Shamanian, and F. Ashrafizadeh, Band gap tuning of oxygen vacancy-induced Al2O3-TiO2 ceramics processed by spark plasma sintering, J. Electroceramics 48(1) (2022) 35–50. doi: 10.1007/s10832-021-00273-4.
[50] L. Zheng *et al.*, Fabrication of ZnO Ceramics with Defects by Spark Plasma Sintering Method and Investigations of Their Photoelectrochemical Properties, Nanomaterials 11(10) (2021) 2506. doi: 10.3390/nano11102506.
[51] Y. Feng, H. Hou, B. Yang, B. Yang, and F. Zi, Decomposition of solid alumina in the presence of carbon in vacuum, Vacuum 145 (2017) 169–173. doi: https://doi.org/10.1016/j.vacuum.2017.08.043.
[52] D. Travessa and M. Ferrante, The Al2O3-t itanium adhesion in the view of the diffusion bonding process, J. Mater. Sci. 37(20) (2002) 4385–4390. doi: 10.1023/A:1020669022776.
[53] Heikinheimo, L. S. K., Interface structure and fracture energy of Al2O3-Ti joints, Phd Thesis (Research TU/e / Graduation TU/e), Chemical Engineering and Chemistry, Technical Research Centre of Finland (1995). https://doi.org/10.6100/IR436699
[54] X. -A. Zhao, E. Kolawa, and M. Nicolet, Reaction of thin metal films with crystalline and amorphous Al2O3, J. Vac. Sci. Technol. A 4(6) (1986) 3139–3141. doi: 10.1116/1.573642.

Figure Captions

Figure 1. Light microscope images of alumina-zirconium systems after SPS experiments under a load of 4.2 kN at a) 800°C, b) 900°C, c) 1000°C

Figure 2. SEM images of the cross-sections obtained from the zirconium-alumina system bonded by spark plasma sintering method under a load of 4.2 kN at a) 800°C, b) 900°C

Figure 3. SEM-EDX mapping analysis of alumina surface after SPS with zirconium interlayer at 1000°C under a load of 4.2 kN

Figure 4. SEM-EDX analysis of alumina surface after SPS at 1000°C with zirconium interlayer under a load of 3 kN

Figure 5. SEM images of the cross-sections obtained from the titanium-alumina system bonded by spark plasma sintering method at a) 700°C, b) 800°C, c) 900°C

Table Captions

Table 2. Examples of systems for solid-state diffusion bonding alumina ceramics from the literature

Table 2. Experimental data of diffusion bonding performed by the spark plasma sintering method

Table 3. Examples of systems for solid-state diffusion bonding alumina ceramics from the literature

Substrate	Substrate	Interlayer	Temperature [°C]	Pressure [MPa]	Reference
Alumina	AISI 304	Ti	700, 800, 900, 1000	15	[16]
Alumina	AISI 304	Ti/Mo	800	15	[16]
Alumina	AISI 304	Ti/Cu	800	15	[16]
Alumina	Ti6Al4V	Ag-Cu	750	3	[19]
Alumina	AISI 304	$AlH_3/Mg(AlH_4)_2$	400	20	[20]
Alumina	Cu	Ti-0.8La (wt.%)	350	from 22 to 28	[6]
Alumina	Ti6Al4V	Ti	950, 1000		[14]
Alumina	1Cr18Ni9Ti steel		from 750 to 1200	7	[21]
Alumina	Alumina	Alumina nanopowder	1100	80	[22]
Alumina	Kovar	Al	540	75	[15]
Alumina	TNZ alloy		1175	3	[23]
Alumina	Alumina		1500	69	[24]
Alumina	Ni		1390	4	[25]
Alumina	Cu		1040	5	[13]
Alumina	Pt		1200	1.8	[26]
Alumina	Nb		from 1500 to 1800	from 3 to 15.2	[27]

Table 2. Experimental data of diffusion bonding performed by spark plasma sintering method

Interlayer	Force [kN]	Temperature [°C]	Heating rate [°C/min]	Dwell time [min]
Titanium	3.0	600	60	15
Titanium	3.0	700	60	15
Titanium	3.0	800	60	15
Titanium	3.0	900	60	15
Zirconium	3.0	800	60	15
Zirconium	3.0	900	60	15
Zirconium	3.0	1000	60	15
Zirconium	4.2	800	60	5
Zirconium	4.2	900	60	5
Zirconium	4.2	1000	60	5

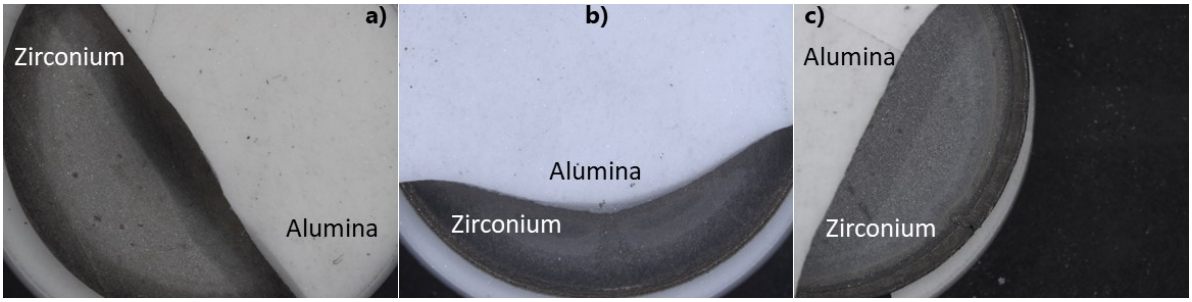

Figure 1. Light microscope images of alumina-zirconium systems after SPS experiments under a load of 4.2 kN at a) 800°C, b) 900°C, c) 1000°C

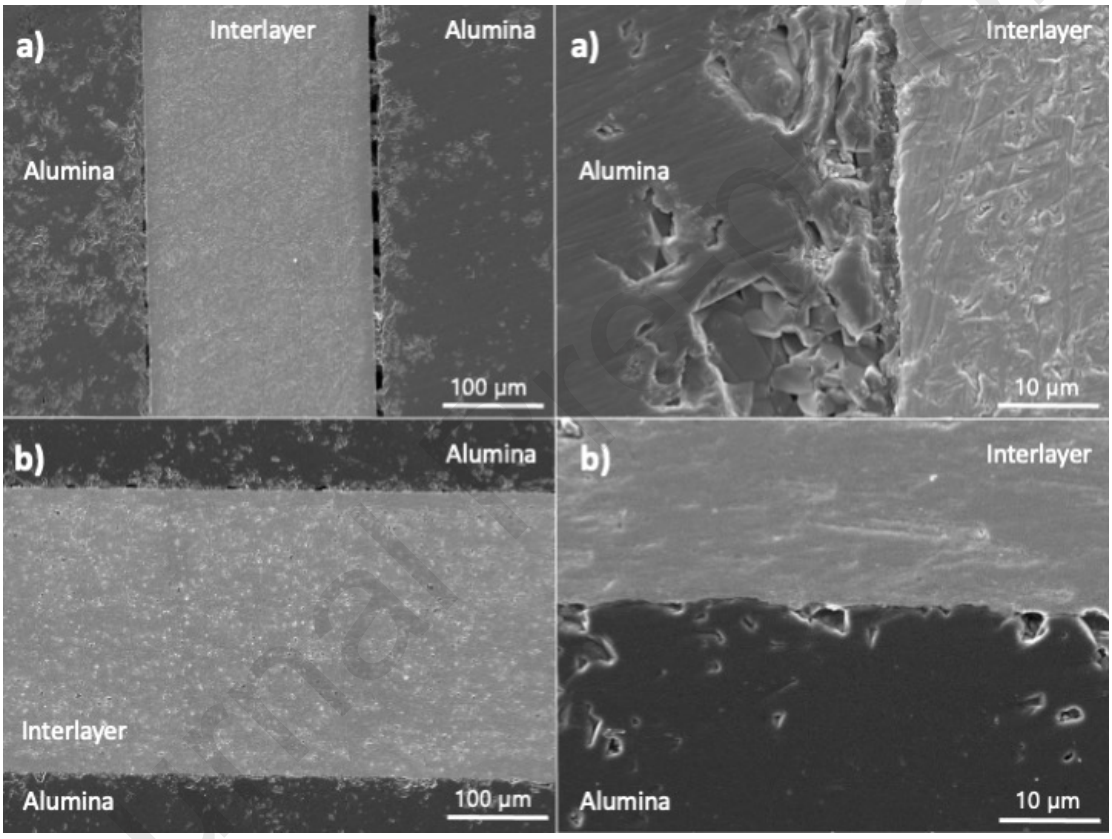

Figure 2. SEM images of the cross-sections obtained from the zirconium-alumina system bonded by spark plasma sintering method under a load of 4.2 kN at a) 800°C, b) 900°C

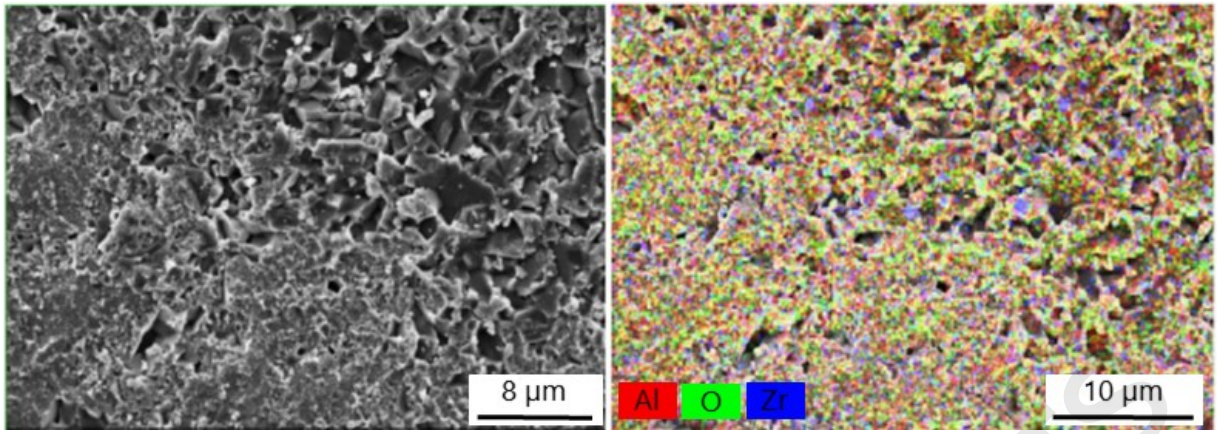

Figure 3. SEM-EDX mapping analysis of alumina surface after SPS with zirconium interlayer at 1000°C under a load of 4.2 kN

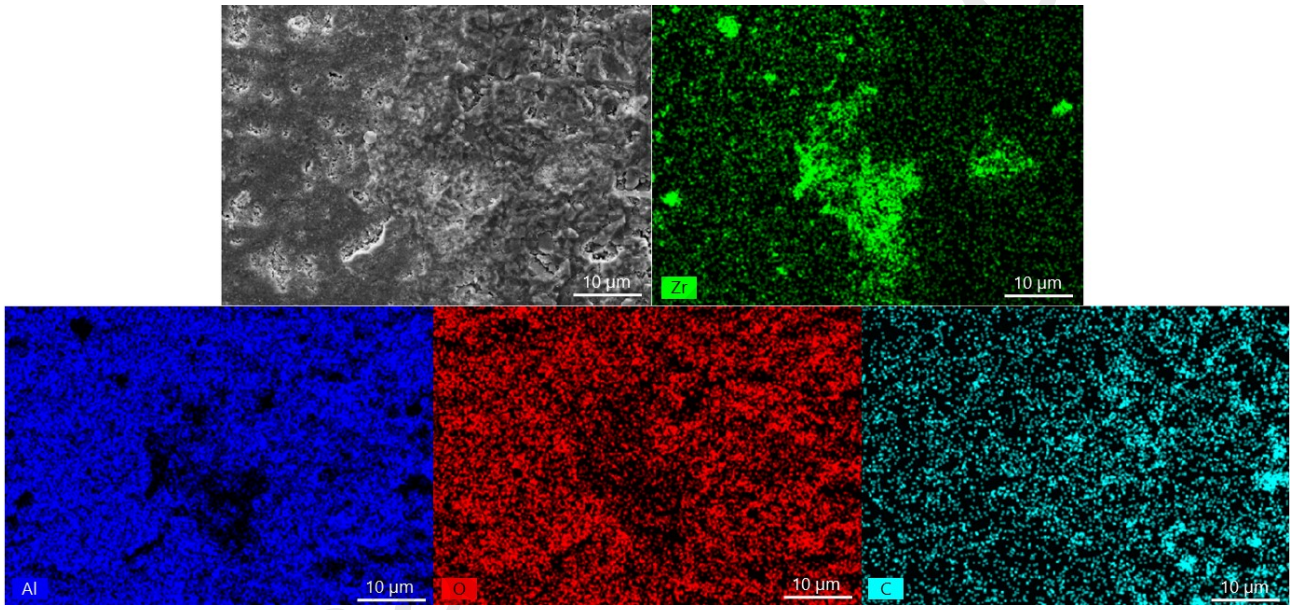

Figure 4. SEM-EDX analysis of alumina surface after SPS at 1000°C with zirconium interlayer under a load of 3 kN

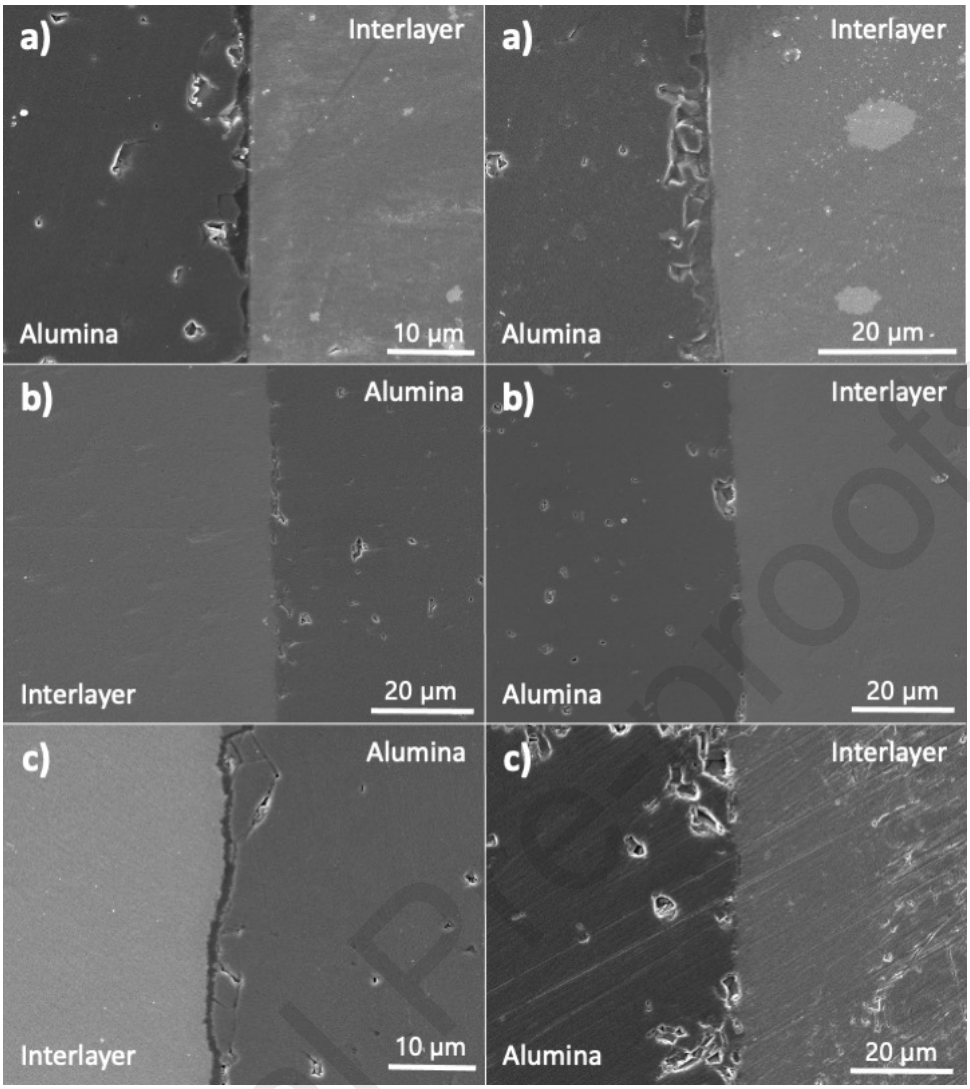

Figure 5. SEM images of the cross-sections obtained from the titanium-alumina system bonded by spark plasma sintering method at a) 700°C, b) 800°C, c) 900°C

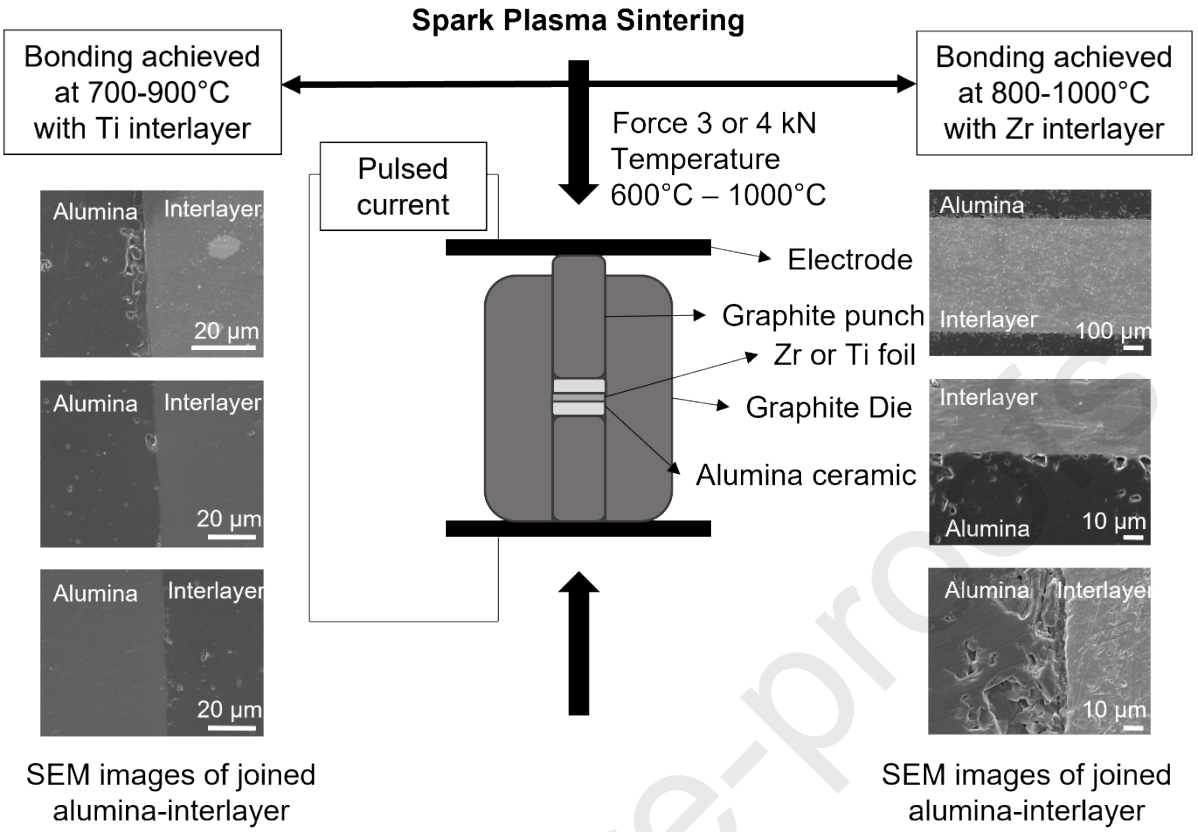

Highlights

- In this study, alumina ceramics were joined by Spark Plasma Sintering (SPS) technology with titanium and zirconium metals applied as interlayers. In the current state of art, titanium successfully joined alumina by SPS for the first time, while bonding with zirconium was not previously mentioned in the literature.
- Titanium joined with alumina at 700, 800, and 900°C (force 3 kN), however, the bond from 800°C stands out with the highest integrity and stability among others. The formation of oxides and metallic compounds are the expected result of the SPS treatment.
- Zirconium-alumina bonding was achieved at 800, and 900°C (force 4.2 kN). The higher temperature resulted in the better quality of bonding, but worse than the titanium systems. The ZrO_2 formation could decrease the stability in the joined system.

Declaration of interests

☒ The authors declare that they have no known competing financial interests or personal relationships that could have appeared to influence the work reported in this paper.

☐The authors declare the following financial interests/personal relationships which may be considered as potential competing interests: